

Water and Glucose Gradients in the Substrate Measured with NMR Imaging During Solid-State Fermentation with *Aspergillus oryzae*

Frank-Jan Nagel,¹ Henk Van As,^{2,3} Johannes Tramper,¹ Arjen Rinzema^{1,4}

¹Wageningen University, Department of Agrotechnology and Food Sciences, Food and Bioprocess Engineering Group, P.O. Box 8129, 6700 EV Wageningen, The Netherlands; telephone: +31-317-484372; fax +31-317-482237; e-mail: arjen.rinzema@algemeen.pk.wau.nl

²Wageningen University, Department of Agrotechnology and Food Sciences, Laboratory of Biophysics, Wageningen, The Netherlands

³Wageningen University and Research Centre, Wageningen NMR Centre, Wageningen, The Netherlands

⁴Wageningen Centre for Food Sciences, Wageningen, The Netherlands

Received 29 March 2001; accepted 6 March 2002

DOI: 10.1002/bit.10332

Abstract: Gradients inside substrate particles cannot be prevented in solid-state fermentation. These gradients can have a strong effect on the physiology of the microorganisms but have hitherto received little attention in experimental studies. We report gradients in moisture and glucose content during cultivation of *Aspergillus oryzae* on membrane-covered wheat-dough slices that were calculated from ¹H-NMR images. We found that moisture gradients in the solid substrate remain small when evaporation is minimized. This is corroborated by predictions of a diffusion model. In contrast, strong glucose gradients developed. Glucose concentrations just below the fungal mat remained low due to high glucose uptake rates, but deeper in the matrix glucose accumulated to very high levels. Integration of the glucose profile gave an average concentration close to the measured average content. On the basis of published data, we expect that the glucose levels in the matrix cause a strong decrease in water activity. The results demonstrate that NMR can play an important role in quantitative analysis of water and glucose gradients at the particle level during solid-state fermentation, which is needed to improve our understanding of the response of fungi to this nonconventional fermentation environment. © 2002 Wiley Periodicals, Inc. *Biotechnol Bioeng* 79: 653–663, 2002.

Keywords: *Aspergillus oryzae*; solid-state fermentation; NMR imaging; gradients; water activity; glucose; diffusion model

INTRODUCTION

Solid-state fermentation (SSF) is defined as the growth of microorganisms, usually fungi, on a solid substrate in

the absence of free-flowing water and in a continuous gas phase. For several biotechnological products, this cultivation method gives superior results compared to submerged fermentation (Nagel et al., 2001a; Oostru et al., 2000). Very little is known about the mechanistic background of the observed differences between SSF and submerged fermentation, although it is known that gene expression in SSF can differ from that in submerged cultures (Hata et al., 1998; Ishida et al., 1998). In Asia, SSF is used on an industrial scale to produce enzymes, such as amylases and proteases, for hydrolysis of vegetable protein and starch during production of fermented foods, such as soy sauce, tempe, miso, and sake (Steinkraus, 1995). Application in Western countries is still unusual because there is insufficient insight into the mechanisms that determine microbial behavior in SSF and a lack of well-established scale-up strategies.

A well-known problem in SSF is simultaneous control of temperature and moisture content of the solid substrate (Lonsane et al., 1992; Nagel et al., 2001b; Ryoo et al., 1991; Saucedo-Castaneda et al., 1992): on an industrial scale, temperature can only be controlled by evaporative cooling, which will result in a decrease in moisture content of the solids over time. The moisture loss is aggravated by the uptake of water in new microbial cells (Nagel et al., 2001b). Simultaneously, extracellular microbial enzymes cause accumulation of monomers, such as sugars (Nagel et al., 2001b). The water loss and solute accumulation will result in a decrease in water activity, which can have beneficial effects on metabolism (Gervais, 1990) but can also result in process failure (Nagel et al., 2001a).

The aim of the work described in this article is to show the effect of fungal growth on gradients inside the

Correspondence to: A. Rinzema

Contract grant sponsor: Dutch Graduate School on Process Technology

substrate particles. The microorganism grows primarily near the outer surface of the substrate particle, due to oxygen supply limitations (Oostra et al., 2001). The water uptake in new biomass and the evaporation are thus both localized at the particle surface, which will cause a moisture gradient in the particles. Furthermore, inhomogeneous distribution of microbial enzymes and uptake of sugars by the microorganisms will cause solute gradients. Intra-particle solute and moisture gradients have hitherto not been taken into account in physiological studies of SSF because it is difficult to control and measure them.

We have used nuclear magnetic resonance imaging (MRI) to obtain spatially resolved moisture and glucose content measurements at the particle level during cultivation of *Aspergillus oryzae* on wheat dough slices. MRI allows non-destructive and non-invasive spatially resolved measurements in SSF systems at the particle level. NMR signals are characterized by a number of different parameters (Hills, 1998): the amplitude A is a direct measure of the amount of water in a sample. Two relaxation times (T_1 and T_2) of the excited nuclear spin system both correlate with the physical state of water in the sample (Van As and Lens, 2001; Van As and van Dusschoten, 1997).

We show that both relaxation times (T_1 and T_2) linearly correlate with glucose and moisture content and that these correlations can be combined to calculate glucose and moisture content profiles in the dough from NMR images. Water profiles in the dough calculated from the NMR images are compared to predictions of a mathematical model that describes water diffusion in the solid substrate driven by a constant water-uptake rate at the surface. Finally, the profiles for glucose and moisture content were used to estimate the water activity profile in the solid substrate.

WATER-DIFFUSION MODEL

During growth of a fungus on the surface of a slab of solid substrate, the water content of the slab will decrease due to water uptake in new fungal cells and—depending on the mode and scale of operation—evaporation. The water loss at the top of the slab causes a concentration gradient in the substrate slab, which results in diffusion of water from lower positions in the substrate to the top. The resulting concentration gradient is calculated by solving the water mass balance with a numerical approximation based on the method of lines. This calculation is complicated by the fact that the water loss will also cause shrinkage of the substrate (Oostra et al., 2000; Weber et al., 1999, 2002). We take this into account by reducing the grid distance in the method of lines, in accordance with the water loss. We assume that the solids and solutes do not diffuse in the

matrix and that the average density of the solids/water mixture can be calculated with a simple additive model. The water-diffusion model is explained below.

Change in Water Content

The mass balance for water in an infinitesimal slice of the substrate slab reads

$$\frac{\partial}{\partial t}(\rho x_1 dz) = -\frac{\partial J_1''}{\partial z} dz \quad [\text{kg} \cdot \text{m}^{-2} \cdot \text{s}^{-1}] \quad (1)$$

or

$$\rho dz \frac{\partial x_1}{\partial t} + x_1 \frac{\partial}{\partial t}(\rho dz) = -\frac{\partial J_1''}{\partial z} dz \quad [\text{kg} \cdot \text{m}^{-2} \cdot \text{s}^{-1}], \quad (2)$$

where ρ is the density of the substrate matrix, i.e., the mixture of solids and water (kg m^{-3}), x_1 is the mass fraction of water, J_1'' is the water flux ($\text{kg m}^{-2} \text{s}^{-1}$), t is the time (s), z is the direction perpendicular to the slice surface (m), and dz is the slice thickness (m). At the top surface, where the fungus grows, we define $z = 0$. The density of the substrate matrix depends on the moisture content.

The first term on the left-hand side in Eq. (2) represents the change in composition; the second, the shrinkage of the slice. The shrinkage can be found from the mass balance for all components together, as explained in the next section. We assume that there is no flux of solids and solutes, which implies that the loss of dry matter due to fermentation is neglected. This is further discussed in the Results and Discussion. The mass balance for all components together reads

$$\frac{\partial}{\partial t}(\rho dz) = -\frac{\partial J_1''}{\partial z} dz \quad [\text{kg} \cdot \text{m}^{-2} \cdot \text{s}^{-1}]. \quad (3)$$

Substitution of Eq. (3) into Eq. (2) gives

$$\frac{\partial x_1}{\partial t} = \frac{(1 - x_1)}{\rho} \left(-\frac{\partial J_1''}{\partial z} \right) \quad [\text{s}^{-1}]. \quad (4)$$

The flux J_1 follows from Fick's first law:

$$J_1'' = -D \frac{\partial}{\partial z}(\rho x_1) \quad [\text{kg} \cdot \text{m}^{-2} \cdot \text{s}^{-1}]. \quad (5)$$

If we neglect any influence of the matrix composition on the diffusion coefficient, Eqs. (4) and (5) give the change in mass fraction of water:

$$\frac{\partial x_1}{\partial t} = D \frac{(1 - x_1)}{\rho} \frac{\partial^2}{\partial z^2}(\rho x_1) \quad [\text{s}^{-1}]. \quad (6)$$

The boundary conditions for Eq. (6) are

$$z = 0 \quad D \frac{d}{dz}(\rho x_1) = J_1''_{1,0} \quad (7)$$

and

$$z = L(t) \quad \frac{d}{dz}(\rho x_1) = 0. \quad (8)$$

Shrinkage

The mass balance for the dry matter over an infinitesimal slice can be used to find the change in slice thickness dz . We assume that there is no flux of solids or solutes, so this mass balance reads

$$\frac{\partial}{\partial t}(\rho x_2 dz) = 0, \quad (9)$$

where x_2 is the weight fraction of dry matter. Taking into account that $x_1 + x_2 = 1$, this gives

$$\rho(1 - x_1) \frac{\partial}{\partial t}(dz) = dz \left(\rho - (1 - x_1) \frac{\partial \rho}{\partial x_1} \right) \frac{\partial x_1}{\partial t}. \quad (10)$$

The average density of the slab, ρ , is affected by the composition. Data on oat grains (Oostru et al., 2000) show that the density can be described with a simple additive model:

$$\frac{1}{\rho} = \left(\frac{1}{\rho_1} - \frac{1}{\rho_2} \right) x_1 + \frac{1}{\rho_2}, \quad (11)$$

where ρ_1 is the density of water in (kg m^{-3}). The dry solids density (ρ_2) is defined as the mass of dry solids divided by the volume occupied by dry solids. The dry solids density is assumed to be constant in this model and is calculated from the density of wet wheat dough at various moisture contents, using Eq. (11).

Combination of Eqs. (10) and (11) gives the change in slice thickness

$$\frac{\partial}{\partial t}(dz) = dz \left(\frac{1}{(1 - x_1)} + \left(\frac{\rho}{\rho_1} - \frac{\rho}{\rho_2} \right) \right) \frac{\partial x_1}{\partial t}. \quad (12)$$

Numerical Approximations

Eq. (6) was solved with a Forward-in-Time-Centered-in-Space approximation that takes into account the variation in Δz caused by the shrinkage (Crank, 1975):

$$\begin{aligned} \frac{\Delta x_{1,i}}{\Delta t} &= 2D \times \frac{1 - x_{1,i}}{\rho_i} \\ &\times \frac{\frac{\Delta z_{1,i}}{\Delta z_{1,i+1}} \rho_{i+1} x_{1,i+1} - \left(1 + \frac{\Delta z_{1,i}}{\Delta z_{1,i+1}} \right) \rho_i x_{1,i} + \rho_{i-1} x_{1,i-1}}{\Delta z_{1,i}^2 + \Delta z_{1,i} \Delta z_{1,i+1}}. \end{aligned} \quad (13)$$

For Eq. (12) we used as a discrete solution

$$\begin{aligned} \Delta(\Delta z_i) &= \frac{\Delta z_i}{2} \left[\left(\frac{1}{1 - x_{1,i}} + \left(\frac{\rho_i}{\rho_1} - \frac{\rho_i}{\rho_2} \right) \right) \Delta x_{1,i} \right. \\ &\left. + \left(\frac{1}{1 - x_{1,i-1}} + \left(\frac{\rho_{i-1}}{\rho_1} - \frac{\rho_{i-1}}{\rho_2} \right) \right) \Delta x_{1,i-1} \right]. \end{aligned} \quad (14)$$

In Eqs. (13) and (14), i refers to the slice number and the grid point at the bottom of this slice, $i - 1$ refers to the grid point at the top of this slice, and $i + 1$ refers to the grid point at the bottom of the next slice.

The initial step size was set equal to the distance between two pixels in the NMR image, namely $\Delta z = 2.3438 \times 10^{-4}$ m; the initial slice thickness was $L = 10.078 \times 10^{-3}$ m (44 grid points). The initial water content of the wheat dough was $x_1(t=0) = 0.483$ kg water per kg total weight. The time step used in the simulations was $\Delta t < 0.2 \Delta x^2/D$ s. Errors in the overall water balance were below 0.1% in all simulations.

Water Flux at the Surface

Two values were used for the water flux at the top of the dough slab $J''_{1,10}$, namely, one based solely on water uptake in newly formed fungal cells,

$$J''_{1,0} = X_{W,X} r''_X, \quad (15)$$

and one that, in addition, takes evaporative cooling into account,

$$J''_{1,0} = X_{W,X} r''_X + \frac{r''_X}{Y_{X/O}} \frac{\Delta H_O}{\Delta H_W}. \quad (16)$$

In Eq. (16) it is assumed that all of the metabolic heat generated is used to evaporate water. The moisture content of the fungal biomass ($X_{W,X}$) is 2.08 kg kg^{-1} DM and was previously shown to remain constant during cultivation on wheat dough (Nagel et al., 2001b); r''_X is the rate of increase in biomass dry weight found during cultivation of *A. oryzae* on wheat dough [$\text{kg m}^{-2} \text{ s}^{-1}$], $Y_{X/O} = 0.029 \text{ kg mol}^{-1}$ is the yield coefficient of biomass on oxygen in this system (Nagel et al., 2001b), $\Delta H_O = 450 \text{ kJ mol}^{-1}$ is the reaction enthalpy per mol of oxygen (Roels, 1983), and $\Delta H_W = 2.419 \text{ kJ kg}^{-1}$ is the evaporation enthalpy of water at 35°C (Lide, 1993).

In Eq. (15) metabolic water production, water needed for starch hydrolysis, and water evaporation are neglected. The first two terms were shown to be relatively small (Nagel et al., 2001b); water evaporation was minimized in the experimental set-up for NMR.

Diffusion Coefficient

We assumed that the water diffusion coefficient in the wheat dough is not affected by changes in dough composition. One value was estimated from a relation for the diffusion coefficient of water in gelatinized wheat flour (Andrieu and Stamatopoulos, 1986). For 35°C and the initial moisture content of our dough (0.483 kg water per kg total weight), this gave a diffusion coefficient of $6 \times 10^{-11} \text{ m}^2 \text{ s}^{-1}$. Another value was estimated from published (Furuta et al., 1984) diffusion coefficients in

maltodextrin (partially hydrolyzed starch) solutions, which gave a value of $1.4 \times 10^{-10} \text{ m}^2 \text{ s}^{-1}$ for the temperature and initial water content of our dough.

MATERIALS AND METHODS

¹H-NMR Imaging

Nuclear magnetic resonance imaging (MRI) experiments were carried out with a 0.5 T NMR imager, equipped with an electromagnet (Bruker, Karlsruhe, Germany) and an SMIS console (Guilford, England) operating at 20.35 MHz. An NMR probe with an internal diameter of 4.5 cm and actively shielded gradients (Doty Scientific, Columbia, USA) was fitted in the 14-cm gap of the magnet. Donker et al. (1997) have previously described the applied inversion-recovery multiple-spin echo (IR-MSE) pulse sequence. During the MRI experiment an image was recorded every 2 h, alternatively in normal and perpendicular to normal direction (Fig. 1). In total 19 images were recorded in normal view and 19 images perpendicular to normal, by recording the complex (real and imaginary) signal of 12 echoes at an inter-echo time of 2.7 ms for each image. The repetition time was set to 0.8 s, and each measurement was repeated four times. In the inversion-recovery domain, we used 6 increments of 40 ms. The field of view

was 3 cm × 3 cm, and the images contained 128 × 128 pixels, thus the resolution was 234 μm. To reduce the effects of heterogeneity in the dough, 88 NMR data points obtained at the same height in the dough were averaged.

The obtained data were first filtered with a Gaussian filter (330 Hz per pixel), before fast Fourier transformation and phasing. The real part of the MRI images was fitted simultaneously in the two dimensions, assuming mono-exponential decay for both T_1 and T_2 , and using a fitting routine based on the Marquardt-Levenberg algorithm (Press et al., 1989). Amplitude, T_1 , and T_2 images were obtained by fitting the following function for the decay of the signal intensity on the NMR data (Donker et al., 1997):

$$S_{x,y}(T_{ir}, t) = S_{x,y}(T_{ir} = \infty, t = 0) \cdot \left(1 - 2 \cdot e^{(-T_{ir}/T_{1,x,y})}\right) \cdot e^{(-t/T_{2,x,y})}, \quad (17)$$

where $S_{x,y}(T_{ir}, t)$ is the signal intensity in pixel x, y at time t in the inversion recovery step T_{ir} , $S_{x,y}(T_{ir} = \infty, t = 0)$ is the extrapolated amplitude in pixel x, y at $t = 0$, representing the spin density, T_1 is the longitudinal relaxation time [s], T_2 is the transversal relaxation time [s], T_{ir} is the inversion recovery incrementing delay [s], and t is the time after the soft 90° pulse [s].

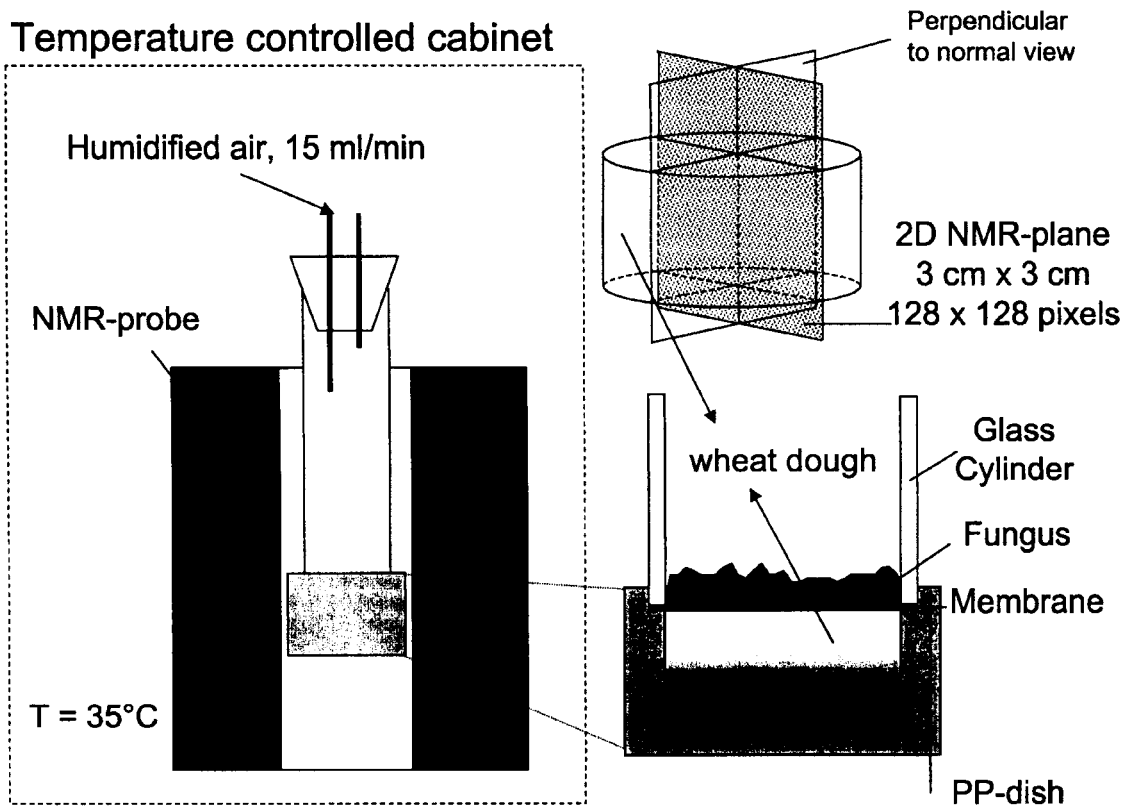


Figure 1. Experimental setup for the MRI experiment, in which *A. oryzae* was cultivated on a wheat-dough model substrate inside the NMR probe. Two dimensional images were recorded every 2 h, alternating in normal view and perpendicular to normal view.

Calibrations

Three wheat dough discs with moisture contents of 0.44, 0.5, and 0.55 kg/kg total and no added glucose were placed together in the NMR system to record amplitude, $1/T_1$, and $1/T_2$ images using the IR-MSE sequence. Each calibration data point was obtained from an average of at least 728 pixels from the MRI images. The same procedure was followed with three wheat discs with different glucose concentrations (0.025, 0.05, and 0.075 kg/kg total) and a moisture content of 0.5 kg/kg total. Calibration measurements were conducted at 28°C. Linear regression analysis was applied to the amplitude data of the MRI images. We assumed that the effects of glucose and moisture content on T_1 and T_2 are not correlated and can be described by the following combination of linear equations:

$$\frac{1}{T_1(x,t)} = \frac{1}{T_1(x,0)} - B_{WT1} \cdot [x_1(x,0) - x_1(x,t)] - B_{GT1} \cdot [x_G(x,0) - x_G(x,t)], \quad (18)$$

$$\frac{1}{T_2(x,t)} = \frac{1}{T_2(x,0)} - B_{WT2} \cdot [x_1(x,0) - x_1(x,t)] - B_{GT2} \cdot [x_G(x,0) - x_G(x,t)], \quad (19)$$

where $T_i(x,t)$ is the relaxation time (T_i) at position x and time t [s], $x_1(x,t)$ is the moisture content at position x and time t [kg kg⁻¹ total], $x_G(x,t)$ is the glucose concentration at position x and time t [kg kg⁻¹ total], B_{WTj} and B_{GTj} are coefficients for moisture content and glucose concentration, respectively [kg total kg⁻¹ s⁻¹], and j is 1 or 2. Regression coefficients B_{WTi} and B_{GTi} were determined using linear regression analysis on either the glucose or moisture data set. The average values for all pixels of both relaxation times at the start of the MRI experiment was used for $1/T_i(x,0)$. The equations were rearranged to allow direct calculation of $x_1(x,t)$ and $x_G(x,t)$ in Figures 7 and 8 from relaxation times.

Microorganism, Substrate, and Incubation

A. oryzae CBS 570.65 was obtained from Centraal Bureau voor Schimmelcultures (Baarn, The Netherlands). A sporangiospore suspension was prepared and utilized for inoculation as described previously (Nagel et al., 2001a). Wheat flour slices (diameter 3 cm, height 1.5 cm) were prepared as described previously (Nagel et al., 2001b). Slices were placed in polypropylene Petri dishes, covered with a sterile 0.45- μ m polyamide membrane (Schleicher & Schuell, NL17 ST), and inoculated with about 3×10^6 spores evenly distributed on top of the membrane. The initial moisture content of the wheat flour slices was 0.483 kg/kg total. One dish was placed in the NMR probe at 35°C (Fig. 1), and several others were placed in a temperature-controlled cabinet at 35°C for

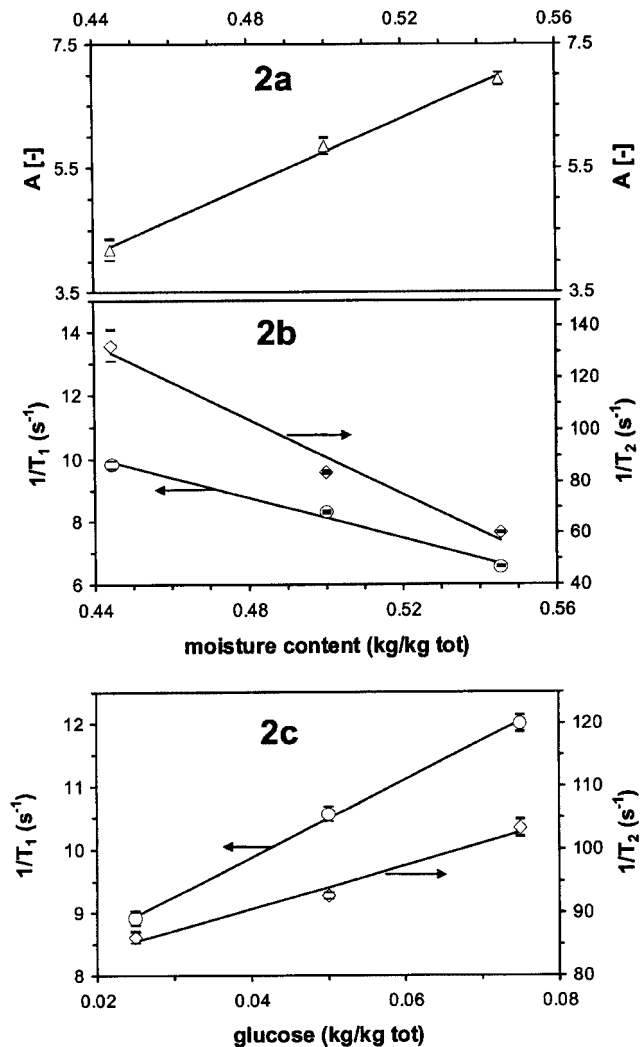


Figure 2. Different wheat discs with variable concentrations of water and glucose were analyzed in the NMR system in order to calibrate NMR parameters A (a, Δ), T_1 (b, \circ), and (c, \diamond) for moisture content and glucose. The solid lines are fitted using linear regression. The horizontal bars represent the standard error in the measurement. The SR-MSE images from which the parameters are calculated are shown in the graphs; the images are turned 90° clockwise with respect to the wheat discs with varying moisture content contain no glucose; moisture content of the wheat discs with varying glucose concentrations is 0.5 kg per kg total weight.

biomass measurements. The dish in the NMR probe was aerated (airflow 15 mL/min, water-saturated at 35°C). The surroundings of the NMR probe were maintained at 35°C with air (30 L/min, RH \approx 50%, $T = 35^\circ\text{C}$).

Analysis

The moisture content of the wheat dough and biomass, the biomass dry weight, and the glucose content of the dough were determined as described previously (Nagel et al., 2001b).

Water Activity

The water activity profile was calculated from the glucose and moisture concentrations using the Ross equation (Ross, 1975):

$$a_w(\text{mixture } m, n \text{ components}) = a_w(1) \cdot a_w(2) \dots \cdot a_w(n), \quad (20)$$

where $a_w(i)$ is the water activity in the binary mixture with component i . In our work this is either a water-glucose mixture or a cooked mixture of water and wheat flour. Moisture contents were converted to water activities using a desorption isotherm for wheat (Nagel et al., 2001b); glucose concentrations were converted to water activities using data of Bonner and Breazeale (1965).

RESULTS AND DISCUSSION

Calibrations

NMR signals are characterized by a number of different parameters. The aim of the calibration was to quantitatively relate the parameters A ($= S_{x,y}[T_{ir} = \infty, t=0]$, Eq. [17]), $1/T_1$, and $1/T_2$, deduced from NMR images to the glucose concentration and moisture content. Figure 2 shows the results of the calibration measurements. Table I shows the regression constants obtained by fitting Eqs. (18) and (19). The first relaxation time (T_1) is more sensitive to glucose content, and the second relaxation time (T_2) is more sensitive to moisture content. The combination of T_1 and T_2 allows the calculation of moisture and glucose concentrations. Apart from the effect of glucose, no additional effect of starch breakdown was observed in calibration measurements with dough incubated with amylase (results not shown).

Growth Experiments

A. oryzae was cultivated on wheat dough in a membrane model system (Nagel et al., 2001b). After a lag phase of

Table I. Calibration of the time constants T_1 and T_2 against glucose content and water content of wheat dough, and of the amplitude A against water content. Values in brackets are standard errors.

Parameter	Value	r^2
Regression analysis of T_1 and T_2 data versus water and glucose content (Eqs. [18] and [19])		
$1/T_1(x,0)$	7.358	
B_{WT1}	-32.3 (3.2)	0.981
B_{GT1}	61.6 (2.4)	0.997
$1/T_2(x,0)$	103.733	
B_{WT2}	-720.4 (100.3)	0.962
B_{GT2}	343.6 (45.5)	0.966
Regression analysis of amplitude data versus moisture content ($x_1 = C_A + B_A A$)		
B_A	0.037 (0.002)	0.993
C_A	0.29 (0.01)	

about 29 h, a linear increase in biomass dry weight ($5.8 \times 10^{-3} \text{ kg m}^{-2} \text{ h}^{-1}$) was found (Fig. 3), which is in agreement with results of previous experiments with this system (Nagel et al., 2001b). The relative standard deviation was 17% for three experiments. From this biomass formation rate, we calculated a water flux at the surface of $1.2 \times 10^{-2} \text{ kg m}^{-2} \text{ h}^{-1}$ for use in the diffusion model.

In order to study water-content gradients in the solid substrate during SSF, *A. oryzae* was cultivated for 3 days on a slice of wheat dough covered with a membrane, inside the NMR probe (Fig. 1). Figure 4 shows MRI images in normal view with a 12-h interval. The images perpendicular to normal view gave similar results. Figures 5 and 6 show T_1 and T_2 values obtained from these images as a function of substrate depth and time. The T_1 images in Figure 4 show a clear gradient, and the fungus (located on the right hand side of the images) is clearly visible. The measurement of T_1 is quite sensitive: the profile at $t = 0$ shows the absorption of the inoculation liquid. High T_2 values are observed near the membrane where the fungus is present. This is explained by the fact that the moisture content of fungal biomass is twice that of the solid substrate and that T_2 is much more sensitive to moisture content (Table I) than to glucose content. The T_2 images display high heterogeneity; nevertheless, a gradient in T_2 can be observed. The amplitude images do not show much variation during the course of fermentation. These images are not homogeneous, which is an indication of heterogeneity in solids composition in the dough. The scatter that is observed mainly in A and T_2 is probably due to inhomogeneous spatial distribution of dough components, flour particle size distribution, and problems that are intrinsic to NMR imaging of systems with low moisture content. In such systems, part of the water is strongly bound to the substrate matrix and exhibits a different relaxation behavior. This results in short T_2 values,

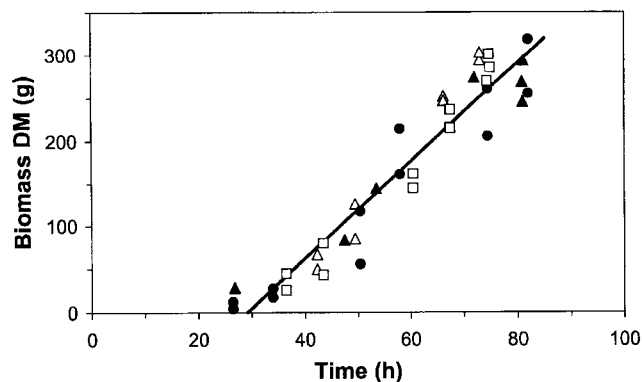


Figure 3. Biomass production during four different cultivations of *A. oryzae* on the membrane model system (Nagel et al., 2001b). The biomass production rate ($5.8 \times 10^{-3} \text{ kg m}^{-2} \text{ h}^{-1}$) was estimated by linear regression analysis of all data (—).

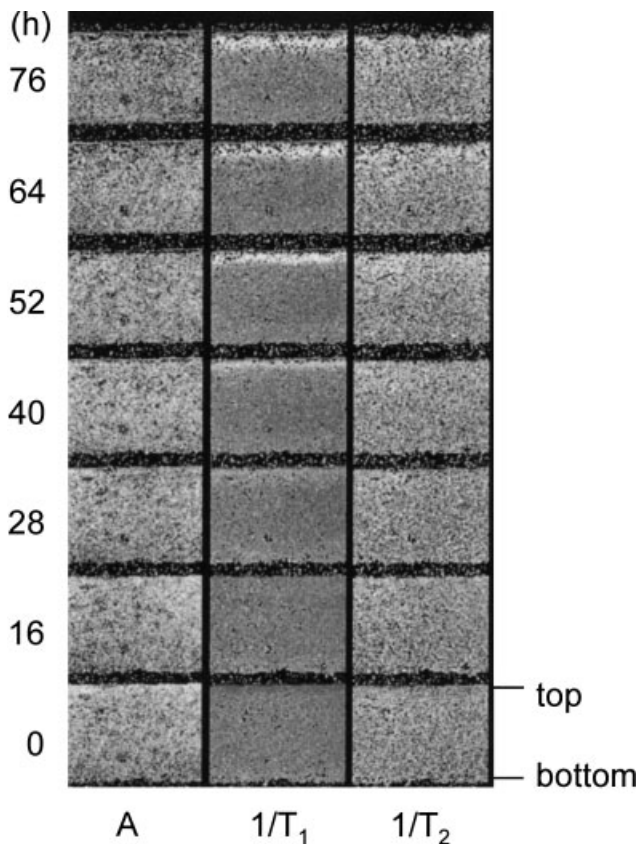


Figure 4. MRI images for amplitude (A) and both reciprocal relaxation times ($1/T_1$ and $1/T_2$) during cultivation of *A. oryzae* on a membrane model system. The time axis is displayed vertically with the cultivation time shown beside the images.

which are difficult to determine accurately. Furthermore, in non-imaging NMR measurements of wheat dough we observed multi-exponential decay for T_2 (data not shown). All MRI measurements were interpreted assuming mono-exponential decay, which may have caused part of the observed scatter.

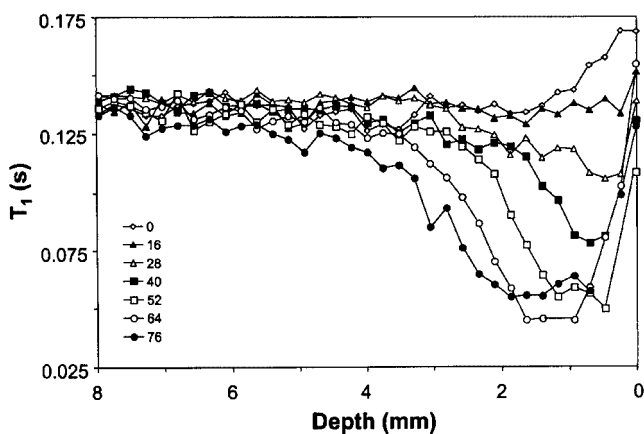


Figure 5. T_1 profile as a function of depth in the wheat dough deduced from MRI images during cultivation of *A. oryzae* on a membrane model system. Numbers in the legend represent the cultivation time in hours. Position 0 indicates the position of the membrane. The presented data do not extend to the bottom of the solid substrate slab.

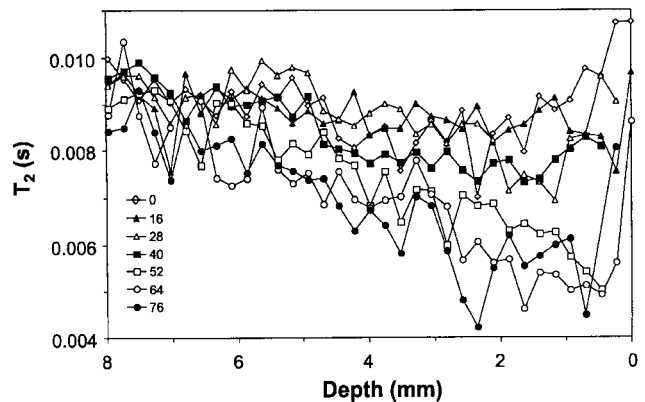


Figure 6. T_2 profile as a function of depth in the wheat dough deduced from MRI images during cultivation of *A. oryzae* on a membrane model system. Numbers in the legend represent the cultivation time in hours. Position 0 indicates the position of the membrane.

Figure 7 shows the glucose content as a function of depth in the wheat dough, calculated from T_1 and T_2 values after 64 h of cultivation time. Just below the top surface the glucose concentration is very low after 64 h, but strong glucose accumulation occurs between 1 and 2 mm depth. The glucose uptake in the fungal mat explains the concentration decrease toward the membrane. The absence of glucose deeper in the matrix indicates that amylolytic enzymes have not yet penetrated beyond a depth of about 2.5 mm after 64 h, which is in accord with the slow diffusion of amylase in a concentrated starch matrix found by Mitchell et al. (1991). The total absence of glucose beyond a depth of about 2.5 mm is surprising, as one would expect diffusion toward the bottom of the dough slice. Further experimental and simulation studies are needed to clarify this observation. The method used to estimate glucose concentrations from the NMR images extended well beyond the range of concentrations for which it has been calibrated. To

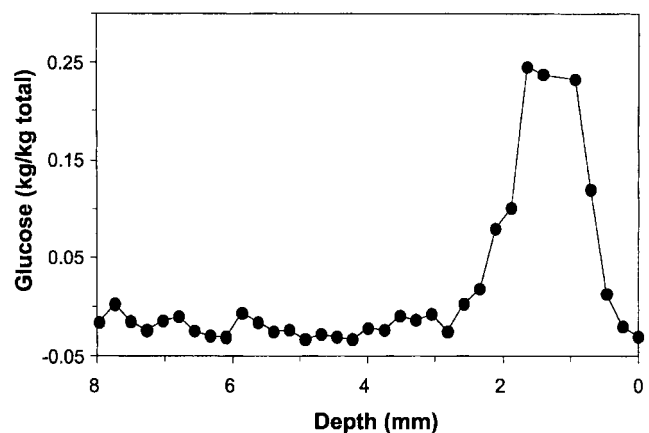


Figure 7. Glucose profile as a function of depth in the wheat dough calculated from both relaxation times (T_1 and T_2) after 64 h cultivation of *A. oryzae* on wheat dough. Position 0 indicates the position of the membrane.

the best of our knowledge no other information is available on the relationship between the relaxation rates $1/T_2$ and $1/T_1$ and the moisture and glucose content in this dough system. The assumptions that the effects of glucose and moisture content on T_1 and T_2 are not correlated and that the calibration on glucose content can be linearly extended to the actually observed range have yet to be verified experimentally by more extended calibrations. These calibrations are expected to be dependent on the actual magnetic field strength B_0 , inter-echo time T_E , the repetition time, and the way the dough is prepared (Hills, 1998). An independent verification of total glucose content gives support to the calculated profile shown in Fig. 7: the average glucose concentration of the whole dough calculated from the glucose profile after 64 h is 0.094 kg per kg DM, which agrees well with the average concentration of 0.092 kg per kg DM (with a relative standard deviation of 8.7%) that was measured after about 64 h in three previous experiments with this model system (Nagel et al., 2001b).

Figure 8 shows a moisture-content profile calculated from T_1 and T_2 values using the combination of Eqs. (18) and (19), and one calculated from amplitude values, both after 64 h cultivation. It is not possible to verify which of the two moisture-content profiles calculated from the NMR data is most realistic due to the scatter in the underlying measurements. The deviation in the moisture content calculated from T_1 and T_2 between 1 and 2 mm depth probably indicates that glucose and moisture content no longer contribute independently to the relaxation behavior at high glucose concentrations.

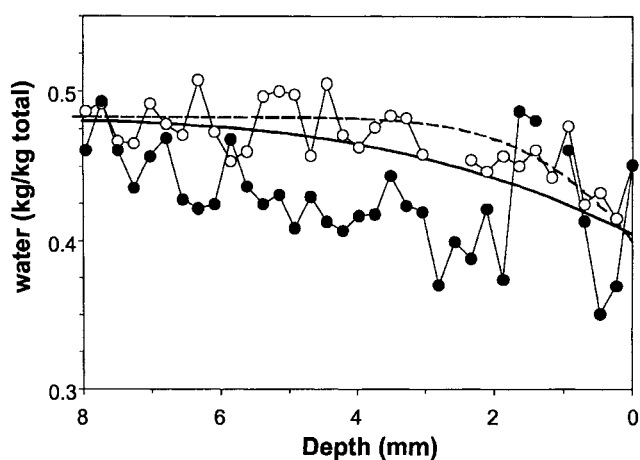


Figure 8. Moisture-content profile as a function of depth in the wheat dough calculated from relaxation times (●) and amplitude (○) after 64 h cultivation of *A. oryzae* on wheat dough. The curved lines represent profiles calculated with the water-diffusion model for 64 h cultivation time with different diffusion coefficients, namely, $D = 6 \times 10^{-11} \text{ m}^2 \text{ s}^{-1}$ (---) and $D = 1.4 \times 10^{-10} \text{ m}^2 \text{ s}^{-1}$ (—), and a water flux at the top surface of $J_{1,0}' = 1.2 \times 10^{-2} \text{ kg m}^{-2} \text{ h}^{-1}$ calculated from the biomass production rate shown in Figure 3. Position 0 indicates the position of the membrane.

The local glucose concentrations found here are far higher than average values found previously that were used to set the calibration interval. With respect to the amplitude, one should note that the high glucose concentrations occurring between 1 and 2 mm depth could cause a (significant) contribution of the protons of glucose to the amplitude measurement.

Two predictions of the water-diffusion model are also shown in Figure 8, which were calculated with different values of the diffusion coefficient and a water flux at the surface of $J_{1,0}' = 1.2 \times 10^{-2} \text{ kg m}^{-2} \text{ h}^{-1}$ calculated from the biomass formation rate (see Fig. 3). For the densities in Eq. (11) we used $\rho_1 = 1,000 \text{ kg m}^{-3}$ and $\rho_2 = 1,564 \text{ kg m}^{-3}$; the latter value was derived from measurements of wet wheat dough density. Considering the scatter in experimental data, the water-diffusion model describes the overall behavior of both measured profiles adequately. This is remarkable, considering that solute diffusion and matrix effects on the diffusion coefficient were neglected.

The simulated profiles and the two experimental profiles show a relatively small moisture-content gradient in the wheat dough, from about 0.5 kg per kg total weight at the bottom of the substrate to about 0.4 kg per kg total weight underneath the membrane. The model predicts a loss of 8.3% of the initial amount of water between 29 and 64 h and a reduction in dough volume of 4.2% of the initial value. Water uptake in new fungal biomass alone does not cause serious moisture shortage during a 64-h cultivation of *A. oryzae* on wheat. This is in agreement with results obtained in fermenters in which evaporation was minimized (Nagel et al., 2001a).

In summary, glucose and moisture-content profiles have been estimated from relaxation times deduced from MRI images. The glucose profile correlates well with a previously measured average glucose concentration, and the moisture profile correlates reasonably with predictions of the water-diffusion model. In the future, the calibration interval of the NMR measurements should be extended to include the extreme values found in this study. Furthermore, the glucose profiles should be validated using independent measurements. This may be done by using microelectrodes or by using fixation, microtome slicing, and chemical analysis.

Water Activity

Besides water, glucose can have a significant effect on the water activity in SSF (Nagel et al., 2001b). Although other solutes might be present in the wheat dough, we believe that glucose is the most important one, given the relative abundance of starch compared to protein in wheat and the high glucose levels measured. Figure 9 shows the combined effect of water and glucose on the water activity after 64 h, calculated with Eq. (20) (Ross,

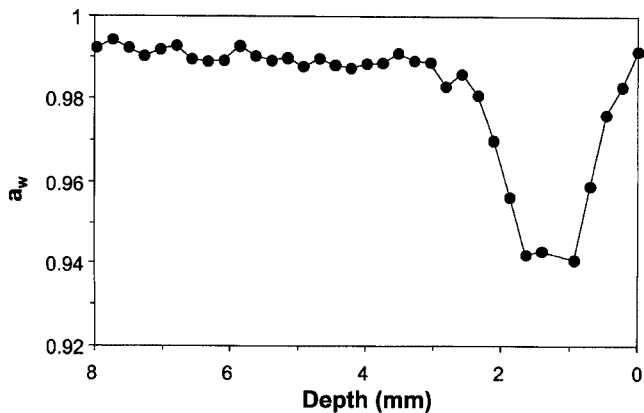


Figure 9. Water-activity profile as a function of depth in the wheat dough calculated using Eq. (20) (Ross, 1975) with glucose and moisture-content profiles after 64 h cultivation of *A. oryzae* on wheat dough. Position 0 indicates the position of the membrane.

1975). Comparison of Figures 7–9 shows that free glucose is mainly responsible for the observed a_w decrease between 1 and 2 mm depth. Immediately below the fungal biofilm, the water activity was not affected due to the glucose uptake into the fungal mat.

An important question is how an SSF culture without a membrane would behave. Hyphae of *A. oryzae* can penetrate into wheat dough at a rate of 0.25 mm h^{-1} , but oxygen diffusion limitation will prevent the mycelium in the dough from reaching the high cell density that is reached in the fungal mat on the surface (Rahardjo et al., in press). Consequently, these penetrating hyphae will not be able to lower the glucose concentration in their vicinity as efficiently as the hyphae in the fungal mat did and will be subjected to a low water activity and low oxygen concentration. This may well trigger physiological responses that contribute to the unique results of SSF reported in literature (Ito, 1993).

The water activity of the solid substrate is one of the most important variables in SSF. It is influenced by a number of biochemical and physical processes, like enzymatic starch hydrolysis, microbial uptake of water and glucose and excretion of metabolites, and evaporation. In order to understand SSF, these processes have to be studied at the particle level. NMR imaging can play an important role in non-invasive studies of gradients caused by these processes. This article shows that moisture- and glucose-content profiles can be determined simultaneously using the combined T_1 and T_2 measurements.

Simulations

Above we used the water diffusion model to verify the moisture-content profile calculated from NMR data. In this section we will discuss (1) predictions of the model for fermentations with evaporative cooling and (2) assumptions and parameter estimates.

Evaporative cooling will drastically increase the amount of water lost from the substrate matrix compared to the loss in the NMR experiment (Nagel et al., 2001b). This implies that the water activity at the particle surface may decrease even when glucose does not accumulate there. The water transport model has been used to simulate the effect of the higher moisture flux at the substrate surface that occurs in case of evaporative cooling, i.e., $J_{1,0}' = 5.1 \times 10^{-2} \text{ kg m}^{-2} \text{ h}^{-1}$ (Eq. [16], Fig. 10). The large difference between local values for water content and water activity at the dough surface and the average values shows that evaporative cooling causes sharp moisture gradients in the wheat dough slab. The model predicts that, after 50 h of evaporative cooling, the moisture content at the wheat dough surface drops below $0.3 \text{ kg per kg total weight}$. This implies that the water activity drops below 0.925 (Nagel et al., 2001a), assuming that fungal activity is not affected and the glucose concentration at the surface remains low due to uptake by the fungus. Such a low water activity would in fact lower the fungal growth rate by 50% (Gibson et al., 1994). This simulation result is in agreement with the observed decline in respiratory activity of the fungus as a result of dehydration during fermentation of wheat in a paddle mixer with evaporative cooling that was reported previously (Nagel et al., 2001a). A more detailed comparison of predictions of the current model to the previously reported results obtained with wheat grains requires that the model be extended to take into account the degradation of substrate dry matter and differences in respiration kinetics

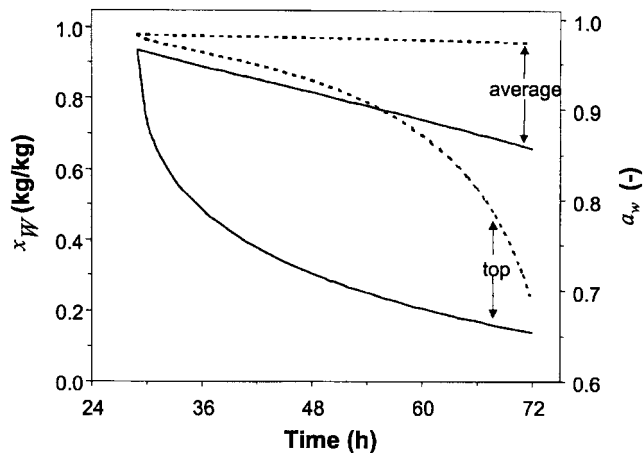


Figure 10. Simulated water content (x_W , solid lines) and water activity (a_w , dashed lines) at the top surface of the dough and on average in the dough, taking into account water uptake in new fungal cells and evaporation (Eq. [16]). The water content was calculated with the water transport model, using a diffusion coefficient of $D = 10^{-10} \text{ m}^2 \text{ s}^{-1}$, a water flux at the top surface of $J_{1,0}' = 5.1 \times 10^{-2} \text{ kg m}^{-2} \text{ h}^{-1}$, and assuming that the fungal activity remains constant. The water activity was calculated from the sorption isotherm of wheat (Nagel et al., 2001b), assuming that there is no solute accumulation. Fungal growth starts after 29 h.

between the wheat dough model substrate and whole grains.

After 64 h of fermentation, the predicted water loss with evaporative cooling is 34.4% of the initial amount of water and the shrinkage is 17.2% of the initial volume; both values are roughly four times higher than those found for the simulations of the situation in which the only mechanism for removal of water from the substrate was incorporation of water into new cells. Shrinkage causes serious problems in unmixed packed beds (Oostra et al., 2000; Weber et al., 1999, 2002). Losses predicted for the dough slab with evaporative cooling are still relatively small compared to those expected for real substrates such as wheat grain (diameter about 4 mm), due to the high initial thickness of the dough slab (height 1.5 cm).

In view of the complexity of the SSF system, models and advanced measurements are needed to elucidate the importance of gradients in the substrate particles. By necessity, such models are simplified. One of the main assumptions made in the current model is that there is no diffusion of glucose or other solutes. Obviously diffusion of solutes could affect the water transport. Extension of the model to include transport of solutes requires the incorporation of a biokinetic model to predict production of low molecular weight solutes such as glucose, which in turn requires the incorporation of fungal growth and enzyme production, transport of oxygen and enzymes, and hydrolysis kinetics. Mitchell et al. (1991) have developed a model that incorporates enzyme release and diffusion, starch hydrolysis, and glucose diffusion and uptake. Current work in our laboratory aims at including these processes in our diffusion model.

Another important simplification in the current model is the use of a constant diffusion coefficient, despite the obvious influence of matrix composition on the diffusion coefficient. This is justified because our primary aims were verification and improvement of understanding, not validation. Furthermore, reduction of the scatter in NMR data and experiments designed to deliver more extreme moisture gradients would be more important than model refinement when validation is aimed for. If matrix effects on the diffusion coefficient are to be included in a future model, these could be verified directly using pulsed field gradient (PFG) NMR (Beuling et al., 1998; Van Dusschoten et al., 1995). The value of spatially resolved diffusivity measurements for the interpretation of measured oxygen concentration profiles has recently been demonstrated for a microbial mat (Wieland et al., 2001).

CONCLUSIONS

¹H-NMR imaging is a powerful technique to study solid-state fermentation non-invasively at the particle level. The water potential of the solid substrate is one of

the most important variables in SSF research and is influenced by a number of biological processes near the biofilm, like enzymatic hydrolysis, water and glucose uptake, and excretion of metabolites. In order to predict and model biomass formation, these processes have to be studied and measured non-invasively on the particle level. This article shows how NMR imaging can play an important role in elucidating complex biological processes.

Water-activity profiles in the solid substrate were estimated during fungal growth, based on moisture-content and glucose profiles calculated from relaxation times deduced from NMR signals. The moisture-content profile was reasonably well predicted with a water-diffusion model, and the glucose profile correlated well with overall glucose measurements.

This article shows that ¹H NMR imaging can be used for quantitative analysis of solid-state fermentation on particle level. Furthermore, this article is a first demonstration of using combined *T*₁ and *T*₂ measurements to measure moisture-content and glucose profiles during solid-state fermentation.

The authors thank M.S.N. Bakker, F. Vergeldt, and P.A. de Jager for assistance with the experiments.

NOMENCLATURE

a_w	water activity	
A	amplitude NMR signal	
B_{WTJ}	regression coefficient in Eq. (18)	
B_{GTJ}	regression coefficient in Eq. (19)	
D	diffusion coefficient	[m ² s ⁻¹]
ΔH_O	reaction enthalpy per mol oxygen	[kJ mol ⁻¹]
ΔH_W	evaporation enthalpy of water at 35°C	[kJ kg ⁻¹]
i	slice or grid number	
J_1''	water flux	[kg m ⁻² s ⁻¹]
$J_{1,0}''$	water flux at top surface	[kg m ⁻² s ⁻¹]
r_X''	biomass production rate	[kg DM m ⁻² s ⁻¹]
$S_{x,y}(T_{ir},t)$	signal intensity in pixel x,y at time t in the inversion recovery step T_{ir}	
t	time	[s]
T_1	longitudinal relaxation time	[s]
T_2	transversal relaxation time	[s]
T_{ir}	Inversion-recovery incrementing delay	[s]
x_1	weight fraction of water	[kg (kg total) ⁻¹]
x_2	weight fraction of dry solids	[kg (kg total) ⁻¹]
x_G	weight fraction of glucose	[kg (kg total) ⁻¹]
$X_{W,X}$	moisture content of biomass	[kg (kg DM) ⁻¹]
$Y_{X/O}$	yield of biomass on oxygen	[kg mol ⁻¹]
z	distance from top surface, along axis perpendicular to surface	[m]
ρ	matrix density	[kg m ⁻³]
ρ_1	density of water	[kg m ⁻³]
ρ_2	density of dry solids	[kg m ⁻³]

References

- Andrieu J, Stamatopolous A. 1986. Moisture and heat transfer modeling during durum wheat pasta drying. In: Mujumdar AS, editor. Drying '86, Vol 2. London: Hemisphere Publishing Corporation.

- Beuling EE, Van Dusschoten D, Lens P, Van den Heuvel JC, Van As H, Ottengraf SPP. 1998. Characterization of the diffusive properties of biofilms using pulsed field gradient nuclear magnetic resonance. *Biotechnol Bioeng* 60:283–291.
- Bonner OD, Breazeale WH. 1965. Osmotic and activity coefficients of some non-electrolytes. *Carbohydrate* 10:325–327.
- Crank J. 1975. *The mathematics of diffusion*, 2nd ed. Oxford: Clarendon Press.
- Donker H, Van As H, Snijder H, Edzes H. 1997. Quantitative ^1H -NMR imaging of water in white button mushrooms (*Agaricus bisporus*). *Magn Reson Imag* 15:113–121.
- Furuta T, Tsujimoto S, Makino H, Okazaki M, Toei R. 1984. Measurement of diffusion coefficient of water and ethanol in aqueous maltodextrin solution. *J Food Eng* 3:169–186.
- Gervais P. 1990. Water activity: a fundamental parameter of aroma production by microorganisms. *Appl Microbiol Biotechnol* 33:72–75.
- Gibson AM, Baranyi J, Pitt JI, Eyles MJ, Roberts TA. 1994. Predicting fungal growth: the effect of water activity on *Aspergillus flavus* and related species. *Int J Food Microbiol* 23:419–431.
- Hata Y, Ishida H, Ichikawa E, Kawato A, Suginami K, Imayasu S. 1998. Nucleotide sequence of an alternative glucoamylase-encoding gene (*glab*) expressed in solid-state culture (koji) of *Aspergillus oryzae*. *Gene* 207:127–134.
- Hills BP. 1998. *Magnetic resonance imaging in food sciences*. New York: Chapman & Hall.
- Ishida H, Hata Y, Ichikawa E, Kawato A, Suginami K, Imayasu S. 1998. Regulation of glucoamylase-encoding gene (*glab*) expressed in solid-state culture (koji) of *Aspergillus oryzae*. *J Ferm Bioeng* 86:301–307.
- Ito K. 1993. Studies on the mycelial growth of *Aspergillus oryzae* on rice grain. *J Soc Ferment Bioeng* 71:115–127.
- Lide DR. 1993. *CRC Handbook of chemistry and physics*, 74th ed. Boca Raton, FL: CRC Press.
- Lonsane BK, Saucedo-Castaneda G, Raimbault M, Roussos S, Viniegra-Gonzalez G, Ghildyal NP. 1992. Scale-up strategies for solid-state fermentation. *Proc Biochem* 27:259–273.
- Mitchell DA, Do DD, Greenfield PF, Doelle HW. 1991. A semi-mechanistic mathematical model for growth of *Rhizopus oligosporus* in a model solid-state fermentation system. *Biotechnol Bioeng* 38:353–362.
- Nagel FJI, Tramper J, Bakker MSN, Rinzema A. 2001a. Temperature control in a continuously mixed bioreactor for solid-state fermentation. *Biotechnol Bioeng* 72:219–230.
- Nagel FJI, Tramper J, Bakker MSN, Rinzema A. 2001b. Model for on-line estimation of moisture content during solid-state fermentation. *Biotechnol Bioeng* 72:231–243.
- Oostra J, Tramper J, Rinzema A. 2000. Model-based bioreactor selection for large-scale solid-state cultivation of *Coniothyrium minitans* spores on oats. *Enzyme Microbial Technol* 27:652–663.
- Oostra J, le Comte EP, van den Heuvel JC, Tramper J, Rinzema A. 2001. Intra-particle oxygen diffusion limitation in solid-state fermentation. *Biotechnol Bioeng* 74:13–24.
- Press WH, Flannery BP, Teukolsky SA, Vetterling WT. 1989. *Numerical recipes in Pascal: the art of scientific computing*. Cambridge: Cambridge University Press.
- Roels JA. 1983. *Energetics and kinetics in biotechnology*. Amsterdam: Elsevier.
- Ross KD. 1975. Estimation of water activity in intermediate moisture foods. *Food Technol* 29:26–30.
- Ryoo D, Murphy VG, Karim MN, Tengerdy RP. 1991. Evaporative temperature and moisture control in a rocking reactor for solid substrate fermentation. *Biotechnol Tech* 5:19–24.
- Saucedo-Castaneda G, Lonsane BK, Raimbault M. 1992. Maintenance of heat and water balances as a scale-up criterion for the production of ethanol by *Schwanniomyces castellii* in a solid-state fermentation system. *Proc Biochem* 27:97–107.
- Steinkraus KH. 1995. *Handbook of indigenous fermented foods*, 2nd ed. New York: Marcel Dekker, Inc.
- Van As H, Lens P. 2001. Use of ^1H NMR to study transport processes in porous biosystems. *J Ind Microbiol Biotechnol* 26:43–52.
- Van As H, Van Dusschoten D. 1997. NMR methods for imaging of transport processes in microporous systems. *Geoderma* 80:389–403.
- Van Dusschoten D, De Jager P, Van As H. 1995. Extracting diffusion constants from echo-time-dependent PFG NMR data using relaxation-time information. *J Magn Reson Ser A* 116:22–28.
- Weber FJ, Tramper J, Rinzema A. 1999. A simplified material and energy balance approach for process development and scale-up of *Coniothyrium minitans* conidia production by solid-state cultivation in a packed-bed reactor. *Biotechnol Bioeng* 65:447–458.
- Weber FJ, Oostra J, Tramper J, Rinzema A. 2002. Validation of a model for process development and scale-up of packed-bed solid-state bioreactors. *Biotechnol Bioeng* 77:381–393.
- Wieland A, Van Dusschoten D, Damgaard LR, De Beer D, Kühl M, Van As H. 2001. Fine-scale measurement of diffusivity in a microbial mat with NMR imaging. *Limnol Oceanogr* 46:28–259.